CIEP 2000
Acapulco, MEXICO
October 15 – 19

Comparison Between Air-Core and Laminated Iron-Core Inductors in Filtering Applications for Switching Converters

U. Reggiani, G. Grandi, G. Sancineto, and G. Serra

Dept. of Electrical Engineering
University of Bologna
Viale Risorgimento 2, 40136 - Bologna, Italy

Abstract – Inductors for filtering devices are widely employed in power electronics applications in order to reduce voltage and current harmonics caused by switching converters. The use of ferrite-core inductors is limited to small power applications, whereas air-core and laminated iron-core inductors are employed in the medium-to-high power range. The choice of the core medium strongly affects the behavior of the inductor versus frequency. In particular, the inductance, the self-resonant frequency, the winding and core losses and the stray magnetic field are quite different for air-core and laminated iron-core inductors. In this paper a comparison between these two kinds of inductors is carried out through an analytical approach and experimental validations.

I. Introduction

In many power filtering devices, both air-core and laminated iron-core inductors are widely employed instead of ferrite-core inductors. The use of ferrite as a core medium offers some advantages, such as lower copper losses compared to air-core inductors and lower core losses compared to laminated iron-core inductors. In addition, the low electric conductivity limits the eddy currents and allows the ferrite-core inductors to operate properly at frequencies up to several MHz. On the other hand, the use of ferrite is generally restricted to applications requiring reduced core dimensions, such as small-signal high-frequency filters or small-inductance reactors, and the ferrite is quite expensive. Mainly for these reasons, air-core and laminated iron-core inductors are preferred over ferrite-core inductors in the medium-to-high power range.

The HF behavior of ferrite-core inductors has been widely investigated in the literature [1]-[5]. Some results concerning eddy currents and losses at high frequencies in laminations are presented in [6] and [7]. The authors have analyzed the HF behavior of both air-core inductors [8] and [9], and laminated iron-core inductors [10].

In this paper, a comparison between air-core and laminated iron-core inductors is carried out with reference to their HF behavior. In particular, a lumped parameter equivalent circuit is developed and validated by experimental tests. The proposed model allows one to compare the behavior of these two different types of inductors in a wide frequency range.

II. Inductor Model

Both air-core and laminated iron-core inductors can be modeled by the lumped parameter equivalent circuit shown in Fig. 1(a). The physical meaning and value of the circuit parameters (i.e., the total ac resistance R_{ac}, the total inductance L_{ac}, and the total parasitic capacitance C) depend on the type of inductor. These parameters are investigated, together with the parallel resistance R_p, in subsections II A and B for air core and laminated iron-core inductors, respectively. In general, R_{ac} and L_{ac} are dependent on frequency f. The impedance of the inductor model is $\hat{Z}_s = R_s + jX_s$. Fig. 1(b) shows a series equivalent circuit of the two types of inductors, where the equivalent series resistance (ESR) is

$$R_s = \frac{R_{ac} + \omega^2 R_p R_{ac}\left(R_{ac} + R_p\right)C^2 + \omega^4 R_p L_{ac}^2 C^2}{\left(1-\omega^2 L_{ac}C\right)^2 + \omega^2 C^2\left(R_{ac} + R_p\right)^2} \tag{1}$$

and the equivalent series reactance is

$$X_s = \frac{\omega L_{ac}\left(1-\omega^2 L_{ac}C - CR_{ac}^2/L_{ac} + \omega^2 R_p^2 C^2\right)}{\left(1-\omega^2 L_{ac}C\right)^2 + \omega^2 C^2\left(R_{ac} + R_p\right)^2} \tag{2}$$

where $\omega = 2\pi f$. Hence, the equivalent series inductance (ESL) is given by

$$L_s = \frac{X_s}{2\pi f} \tag{3}$$

which is also significant because most network analyzers and impedance meters measure R_s and L_s. The self-resonant frequency f_r of an inductor is defined as the frequency at which its reactance X_s becomes zero. Hence, from (2) the inductor total parasitic capacitance C can be calculated.

A. Air-Core Inductors

For air-core inductors, the total ac resistance R_{ac} coincides with the winding ac resistance R_w, and the total inductance L_{ac} can be considered practically independent of frequency and equal to the total low-frequency inductance L_{dc}.

0-7803-6489-9/00/$10.00© 2000 IEEE

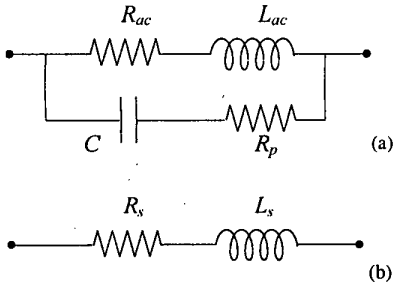

Fig. 1. Equivalent circuits of the two types of inductors: (a) lumped parameter equivalent circuit, (b) series equivalent circuit.

The frequency-dependent parameter R_w is calculated assuming that the leakage magnetic field lines cross the winding in the direction of the coil axis, and neglecting edge effects. An expression for R_w is given by the Dowell's formula [11]

$$R_w = R_{wdc} A \cdot \left[\frac{e^{2A} - e^{-2A} + 2\sin(2A)}{e^{2A} + e^{-2A} - 2\cos(2A)} + 2\frac{N_l^2 - 1}{3} \frac{e^{A} - e^{-A} - 2\sin A}{e^{A} + e^{-A} + 2\cos A} \right] \quad (4)$$

where R_{wdc} is the winding dc resistance, N_l is the numbers of layers of the winding, and A is a unitless quantity, which depends on the winding geometry. The first and second terms of (4) represent the skin effect and the proximity effects in the winding, respectively. For a round wire with conductor diameter d, the quantity A is given by

$$A = \left(\frac{\pi}{4}\right)^{\frac{3}{4}} \frac{d^{\frac{3}{2}}}{\delta_w p^{\frac{1}{2}}} \quad (5)$$

where p is the winding pitch, i.e., the distance between the centers of two adjacent conductors, and δ_w is the skin depth of the wire expressed as

$$\delta_w = \sqrt{\frac{\rho_w}{\pi \mu_o \mu_{rw} f}} . \quad (6)$$

In (6), ρ_w is the wire electric resistivity, μ_{rw} is the wire relative magnetic permeability ($\rho_w = 17.24 \times 10^{-9} \Omega$m and $\mu_{rw} = 1$ for a copper conductor at 20°C), and $\mu_0 = 4\pi\ 10^{-7}$ H/m.

The value of the inductance L_{dc} be calculated by empirical formulas [12] or by an analytical approach [8].

Air-core inductors do not have turn-to-iron stray capacitances. So, only turn-to-turn stray capacitances are considered to evaluate the overall parasitic capacitance C, as described in [8] and [9]. The parallel resistance R_p is introduced to extend the validity of the model above the self-resonant frequency. This resistance accounts for the losses produced in the winding by the HF currents flowing across the dielectric between two turns. R_p is in the order of the tens or hundreds of ohms.

The parameters of interest for two different air-core inductors are reported in Table I. The two inductors have the same number of turns per layer N_l, but different number of layers N_l. In Table I, A_{air} is the cross section area of the air-core and L_{dc} is the total low-frequency inductance.

TABLE I
AIR-CORE INDUCTOR PARAMETERS

	Inductor #1	Inductor #2
d (mm)	1.46	1.46
p (mm)	$p = d$	$p = d$
N_l	8	2
N_t	24	24
A_{air} (mm^2)	1120	1120
R_{wdc} (mΩ)	361.3	73
L_{dc} (mH)	1.6	0.086
f_r (MHz)	0.741	3.877
C (pF)	56	22.24
R_p (Ω)	100	40

Measurements were performed on the two air-core inductors to test the validity of the proposed model. An HP 4192A LF impedance analyzer (5Hz-13MHz) equipped with an HP 16047A test fixture was employed to achieve a higher accuracy by minimizing residual parameters such as contact resistances [13].

Figs. 2 and 3 show the calculated (solid line) and measured (dotted line) equivalent series resistance R_s and reactance X_s of the tested inductor #1 as a function of frequency. The calculated (solid line) and measured (dotted line) equivalent series resistance R_s and reactance X_s of the tested inductor #2 are depicted in Figs. 4 and 5, respectively. It can be seen that the numerical and experimental results are in good agreement.

B. Iron-Core Inductors

In iron-core inductors, owing to the iron high electric conductivity and in spite of the core lamination, the effects produced by the eddy currents in the core are significant starting from frequencies of some tens of kHz. At high frequencies, eddy currents cause additional core losses. Furthermore, the magnetic field in the core is weakened and, consequently, the main inductance decreases. The eddy currents and the corresponding parameters in the inductor model have been evaluated by a one-dimensional electromagnetic field analysis extended to cores with air gaps [10]. In fact, introducing air gaps is the most common way to linearize the behavior of an inductor over a large excursion range of the winding current, avoiding the core saturation and reducing the harmonic distortion.

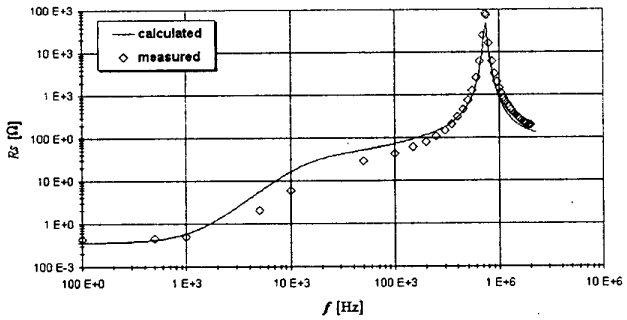

Fig. 2. Calculated and measured equivalent series resistance, R_s, for the air-core inductor #1.

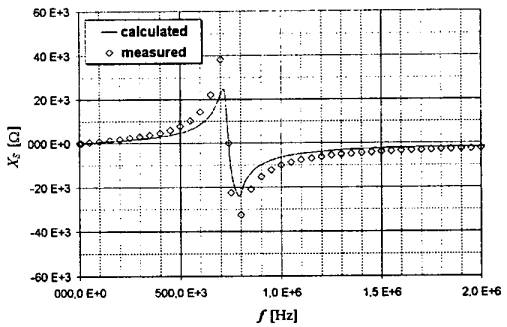

Fig. 3. Calculated and measured equivalent series reactance, X_s, for the air-core inductor #1.

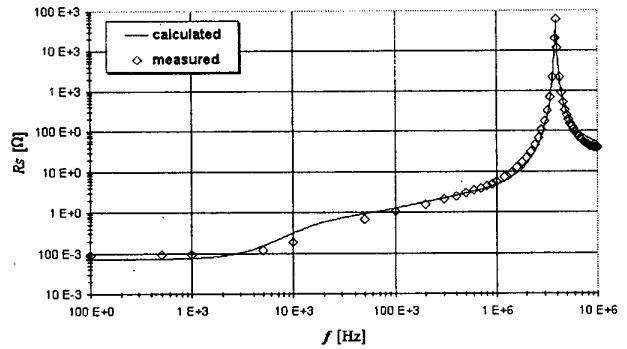

Fig. 4. Calculated and measured equivalent series resistance, R_s, for the air-core inductor #2.

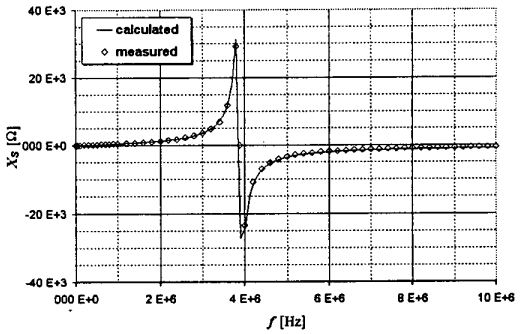

Fig. 5. Calculated and measured equivalent series reactance, X_s, for the air-core inductor #2.

In this case the total ac resistance R_{ac} and the total inductance L_{ac} are given by

$$R_{ac} = R_w + R_c \tag{7}$$

and

$$L_{ac} = L_{ac}^m + L_{ac}^l \tag{8}$$

where R_c is the equivalent series resistance, related to the losses due to eddy currents flowing in the core, L_{ac}^m is the main inductance, related to the paths of the magnetic field lines in the core, and L_{ac}^l is the leakage inductance.

For non-saturated laminated iron-core inductors, the expressions of R_c and L_{ac}^m are [10]

$$R_c = \omega L_{dc}^m \frac{\delta_c}{s} \frac{sinh\frac{s}{\delta_c} - sin\frac{s}{\delta_c}}{\cosh\frac{s}{\delta_c} + \cos\frac{s}{\delta_c}} \tag{9}$$

and

$$L_{ac}^m = L_{dc}^m \frac{\delta_c}{s} \frac{\sinh\frac{s}{\delta_c} + \sin\frac{s}{\delta_c}}{\cosh\frac{s}{\delta_c} + \cos\frac{s}{\delta_c}} \tag{10}$$

where L_{dc}^m is the main inductance at low frequency, s is the thickness of the lamination, and δ_c is the skin depth for the iron sheets given by

$$\delta_c = \sqrt{\frac{\rho_c}{\pi f \mu_e}}. \tag{11}$$

In (11) ρ_c is the electric resistivity of the iron sheets and μ_e is the equivalent permeability of the magnetic circuit with air gaps. The value of μ_e for an EI core is calculated in the following.

In (7) the parameters R_w is calculated by (4). The leakage inductance L_{ac}^l in (8) is dependent on frequency and can be evaluated by the Dowell's approach [11] as

$$L_{ac}^l = R_{wdc} \frac{A}{\omega} \cdot \left[\frac{e^{2A} - e^{-2A} - 2\sin(2A)}{e^{2A} + e^{-2A} - 2\cos(2A)} + 2\frac{{N_l}^2 - 1}{3} \frac{e^A - e^{-A} + 2\sin A}{e^A + e^{-A} + 2\cos A} \right]. \tag{12}$$

In iron-core inductors, the total parasitic capacitance C takes into account the overall effects of turn-to-turn and turn-to-iron stray capacitances. The capacitance C can be calculated as described in [8]. The parallel resistance R_p takes account of the same physical phenomenon considered for air-core inductors.

Two different laminated iron-core inductors were tested. They were arranged by the same EI core depicted in Fig. 6 in order to emphasize the winding contribution.

The value of the equivalent permeability of the EI core was calculated as

$$\mu_e = \mu_c \frac{l_c}{l_c + 2\mu_{rc} l_a} \tag{13}$$

where μ_c is the magnetic permeability of the iron sheets, μ_{rc} is the corresponding relative permeability, l_c is the length of the path consisting of the geometrical axis of the half central limb and that of one of two outer limbs, and $2l_a$ is the total air gap.

The parameters of interest for the two tested inductors are reported in Table II. In this table the low-frequency main inductance L_{dc}^m is indicated instead of the total one because for laminated iron-core inductors the leakage inductance is usually negligible as compared to the main inductance. The low-frequency main inductance is calculated as

$$L_{dc}^m = \mu_e (N_l N_t)^2 \frac{A_{iron}}{l_c} \tag{14}$$

where A_{iron} is the effective cross section area of the central limb. The magnetic permeability of the laminated iron core used in the calculations corresponds to its initial value. The measured relative initial permeability was $\mu_{rci} = 300$. The measured resistivity of the iron sheet was $\rho_c = 7 \times 10^{-7}$ Ωm. The lamination thickness was $s = 0.3$ mm.

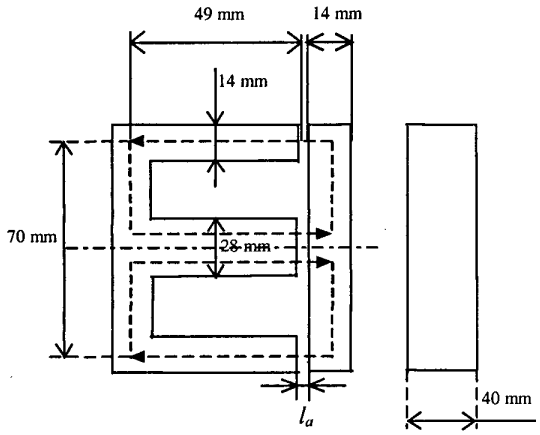

Fig. 6. View of an EI core.

Figs. 7 and 8 show the calculated (solid line) and measured (dotted line) equivalent series resistance R_s and reactance X_s of the tested inductor #3 as a function of frequency. Figs. 9 and 10 depict the calculated (solid line) and measured (dotted line) equivalent series resistance R_s and reactance X_s for the inductor #4. Figs. 7-10 show a good agreement between the calculated and experimental results for the equivalent series parameters.

TABLE II
IRON-CORE INDUCTOR PARAMETERS

	Inductor #3	Inductor #4
d (mm)	1.5	1.46
p (mm)	$p \approx d$	$p \approx d$
N_l	6	2
N_t	23	24
A_{iron} (mm^2)	1067	1067
l_c (mm)	168	168
l_a (mm)	0.4	0.21
μ_e / μ_0	123.5	175
R_{wdc} (mΩ)	236	73
L_{dc}^m (mH)	18.8	3.15
f_r (MHz)	0.103	1.485
R_p (Ω)	150	40

III. COMPARISON IN THE FREQUENCY DOMAIN

In this section a comparison between air-core and laminated iron-core inductors in the HF range is developed. In this paper, among all the possible arrangements of the two kinds of inductors, the authors decided to compare air-core and laminated iron-core inductors having the same winding. This choice allows us to evaluate how the presence of a laminated iron core affects the behavior of the inductor in the HF range. The comparison is made with reference to the air-core inductor #2 and laminated iron-core inductor #4 .

In the following subsections some quantities of interest (i.e., total inductance, total ac resistance, ESL, ESR and quality factor) are calculated and measured for these two inductors. To emphasize the effects of the eddy currents in the iron core, the capacitive branch of the equivalent circuit shown in Fig. 1(a) is not considered in this section. In this way the calculated values do not depend on stray capacitances but the measured ones do. So, comparing the theoretical and experimental results makes possible to point out the frequencies up to which the capacitive effects are negligible.

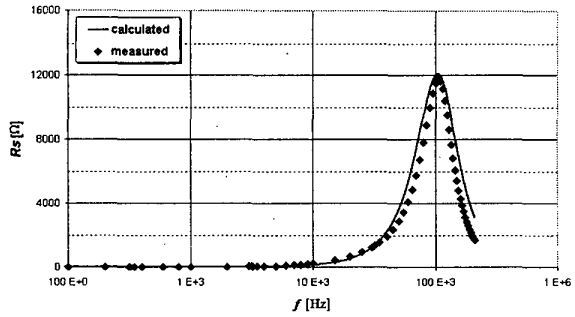

Fig. 7. Calculated and measured equivalent series resistance, R_s, for the iron-core inductor #3.

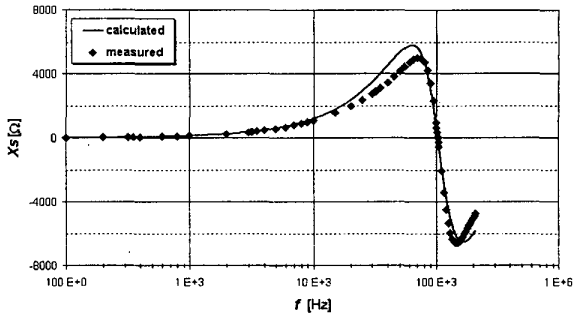

Fig. 8. Calculated and measured equivalent series reactance, X_s, for the iron-core inductor #3.

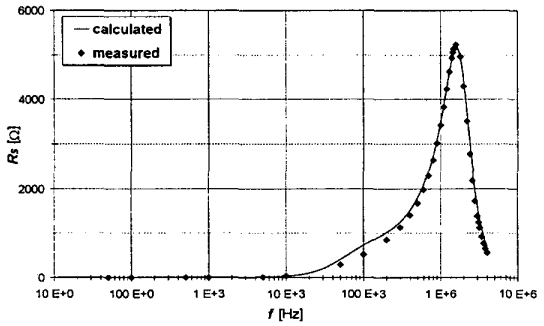

Fig. 9. Calculated and measured equivalent series resistance, R_s, for the iron-core inductor #4.

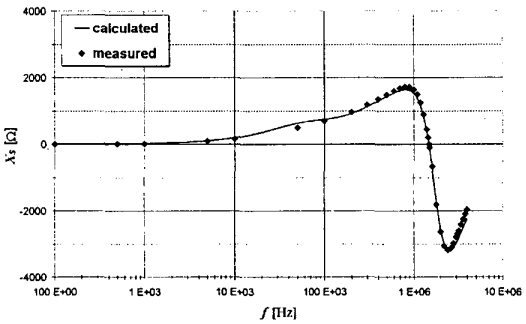

Fig. 10. Calculated and measured equivalent series reactance, X_s, for the iron-core inductor #4.

A. Inductance

The behavior of the total inductance L_{ac} versus frequency is investigated for the two inductors considered. Of course the comparison makes sense if the inductances are normalized with respect to their low-frequency values so that the HF behavior can be emphasized.

Fig. 11 depicts the normalized values of the calculated total inductance L_{ac} and the measured equivalent series inductance L_s as a function of frequency. The calculated curve for the laminated iron-core inductor shows that the decrease of the total inductance L_{ac}, due to the eddy currents in the core, is small up to a few tens of kHz. The measured values of L_s show that the effect of the overall parasitic capacitance of the two inductors is negligible about up to 1 MHz.

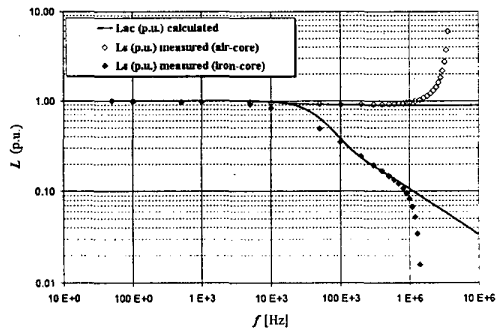

Fig. 11. Calculated total inductance, L_{ac}, and measured equivalent series inductance, L_s, (p.u.).

B. Losses

In this subsection the inductor losses are analyzed in terms of total ac resistance. Fig. 12 shows the behavior of the calculated total ac resistance R_{ac} and the measured equivalent series resistance R_s, normalized with respect to the winding dc resistance, versus frequency.

As expected, the resistance R_{ac} and then the losses increase much more in the laminated iron-core inductor compared to the air-core inductor. In the frequency range from 0.5 to 5 kHz the increase of loss in the laminated iron-core inductor is about from ten to fifty times the one in the air-core inductor.

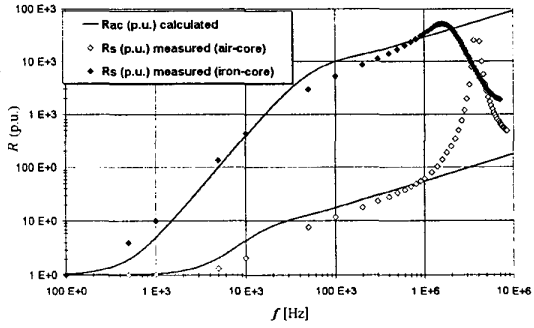

Fig. 12. Calculated total ac resistance, R_{ac}, and measured equivalent series resistance, R_s, (p.u.).

C. Quality Factor

Fig. 13 depicts the calculated quality factor, defined as $Q = \omega L_{ac}/R_{ac}$, and the measured one $Q_s = X_s/R_s$. It can be seen that for frequencies up to a few kHz the laminated iron-core inductor has a higher quality factor and, consequently, realizes a more efficient passive component.

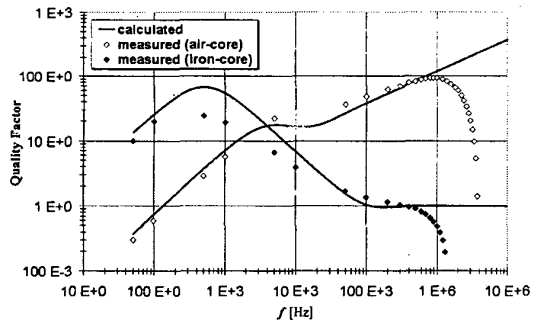

Fig. 13. Calculated and measured quality factor.

IV. CONCLUSIONS

In this paper an HF lumped parameter equivalent circuit for air-core and laminated iron-core inductors is proposed and validated by experimental tests. This model allows one to investigate the HF behavior of these two kinds of inductors. A comparison is carried out in terms of inductance, losses and quality factor as a function of frequency.

For frequencies up to a few kHz the iron-core inductor has to be preferred over the air-core one as its quality factor is higher. On the other hand, the inductance of the iron-core inductor decreases slightly with the increasing frequency. Furthermore, in this frequency range the iron core is a preferential path for the magnetic field lines reducing the magnetic coupling with other parts of the system and, consequently, electromagnetic interferences.

The overall parasitic capacitance of the two considered inductors is almost the same. Hence the presence of the iron core does not practically influence the parasitic capacitance value, which mainly depends on the winding arrangement.

REFERENCES

[1] T. Sato and Y. Sakaki, "Physical meaning of equivalent loss resistance of magnetic cores," *IEEE Trans. Magn.*, vol 26, pp.. 2894-2897, Sept. 1990.

[2] M. Bartoli, A. Reatti, and M.K. Kazimierczuk, "Modeling iron-powder inductors at high frequencies," in *Proc. IEEE IAS Annual Meeting*, 1994, pp.1225-1232.

[3] H. Saotome and Y. Sakaki, "Iron loss analysis of Mn-Zn ferrite cores", *IEEE Trans. Magn*, vol. 33, pp.728-734, Jan. 1997.

[4] D. Zhang and F. Foo, "Theoretical analysis of the electrical and magnetic field distributions in a toroidal core with circular cross section", *IEEE Trans. Magn*, vol. 35, pp. 1924-1931, May 1999.

[5] M.K. Kazimierczuk, G. Sancineto, G. Grandi, U. Reggiani, A, Massarini, "High-frequency small-signal model of ferrite core inductors," *IEEE Trans. Magn*, vol. 35, pp. 4185-4191, Sept. 1999.

[6] L. Rouve, F. Ossart, T. Waeckerlé, A. Kedous-Lebouc, "Magnetic flux and losses computation in electrical laminations," *IEEE Trans. Magn*, vol. 32, pp. 4219-4221, Sept. 1996.

[7] J. Gyselinck, L. Vandevelde, J. Melkebeek, P. Dular, F. Henrotte and W. Legros, " Calculation of eddy currents and associated losses in electrical steel laminations", *IEEE Trans. Magn*, vol. 35, pp. 1191-1194, May 1999.

[8] A. Massarini, M.K. Kazimierczuk, and G. Grandi, "Lumped parameter models of single- and multiple-layer inductors," in *Proc. IEEE PESC*, 1996, pp. 295-301.

[9] G. Grandi, M.K. Kazimierczuk, A. Massarini, and U. Reggiani, "Stray capacitances of single-layer solenoid air-core inductors," *IEEE Trans. Ind. Applicat.*, vol. 35, pp. 1162-1168, Sept./Oct. 1999.

[10] U. Reggiani, G. Grandi, G. Sancineto, M.K. Kazimierczuk, and A. Massarini, "High-frequency behavior of laminated iron-core inductors for filtering applications," in *Proc. IEEE APEC*, 2000, pp. 654-660.

[11] P.J. Dowell, "Effects of eddy currents in transformer windings," *Proc. Inst. Elect. Eng.*, vol. 113, pp. 1387-1394, Aug. 1966.

[12] F.W. Grover, *Inductance Calculations*. New York: D. Van Nostrand Company, Inc., 1947.

[13] M. Honda, *The Impedance Measurament Handbook*. Hewlett Packard Co., 1994.